J.-L. Martin · A. Migus
G. A. Mourou · A. H. Zewail (Eds.)

Ultrafast Phenomena VIII

Proceedings
of the 8th International Conference,
Antibes Juan-Les-Pins, France, June 8–12, 1992

With 523 Figures

Springer-Verlag
Berlin Heidelberg New York
London Paris Tokyo
Hong Kong Barcelona
Budapest

Contents

Part I **Overview and General Prospects**

Additive Pulse Modelocking and Kerr-Lens Modelocking
By H.A. Haus (With 6 Figures) 3

Molecular Control Spectrometer
By Y. Yan, B.E. Kohler, R.E. Gillilan, R.M. Whitnell, K.R. Wilson, and S. Mukamel 8

Internal Motions of Proteins
By M. Karplus 13

Some Theoretical Aspects of Electron Transfer in Supermolecules
By J. Jortner and M. Bixon (With 3 Figures) 15

Femtosecond Time-Resolved Spectroscopy of Magneto-Excitons
By D.S. Chemla, J.B. Stark, and W.H. Knox (With 6 Figures) 21

High-Order Harmonic Generation in Strong Laser Fields
By A. L'Huillier and P. Balcou (With 3 Figures) 29

QED at 10^{20} W/cm^2
By A.C. Melissinos (With 6 Figures) 34

Part II **Elementary Dynamics: Chemistry, Biology and Physics**

Femtochemistry
By A.H. Zewail (With 6 Figures) 43

Transient Dichroism Studies of I_2 Predissociation in Solution
By N.F. Scherer, L.D. Ziegler, D. Jonas, and G.R. Fleming (With 3 Figures) 49

Investigation of the Primary Event in Vision Using 10 fs Blue-Green Optical Pulses
By R.W. Schoenlein, L.A. Peteanu, Q.W. Wang, R.A. Mathies, and C.V. Shank (With 3 Figures) 53

Mechanisms of Charge Separation in Bacterial Reaction Centers
By M.H. Vos, F. Rappaport, J.-C. Lambry, C. Rischel, J. Breton, and J.-L. Martin (With 2 Figures) 58

Coherent Phonons in Superconducting Materials
By W. Albrecht, Th. Kruse, and H. Kurz (With 3 Figures) 63

Displacive Excitation of Coherent Phonons
By T.K. Cheng, J. Vidal, H.J. Zeiger, E.P. Ippen, G. Dresselhaus, and M.S. Dresselhaus (With 1 Figure) 66

Femtosecond Time-Resolved Photodissociation of Triiodide Ions in Alcohol Solution: Directly Observed Photoinduced Vibrational Coherence of Reactants and Products
By U. Banin, A. Waldman, and S. Ruhman (With 4 Figures) 68

Vibrational Coherence in Charge Transfer
By K. Wynne, C. Galli, P.J.F. De Rege, M.J. Therien, and R.M. Hochstrasser (With 1 Figure) 71

Ultrafast Dynamics in Solution:
Wavepacket Motion and the Cage Effect in Iodine
By Y. Yan, R.M. Whitnell, K.R. Wilson, and A.H. Zewail (With 1 Figure) 74

Femtosecond Time-Resolved Ionization Spectroscopy of Polyatomic Molecules
By M. Seel and W. Domcke (With 1 Figure) 76

A Study of Nuclear Vibrational Wave Packets in Na_2 by Time- and Frequency-Resolved Fluorescence Upconversion
By I.A. Walmsley, T.J. Dunn, J. Sweetser, and C. Radzewicz (With 3 Figures) 78

Ultrafast Dynamics of Solid C_{60}
By S.L. Dexheimer, D.M. Mittleman, R.W. Schoenlein, W. Vareka, X.-D. Xiang, A. Zettl, and C.V. Shank (With 2 Figures) 81

Femtosecond Dynamics
of Molecular and Cluster Ionization and Fragmentation
By T. Baumert, R. Thalweiser, V. Weiß, and G. Gerber (With 5 Figures) 83

Dephasing and Beats of Excitonic-Enhanced Transitions of J-Aggregates Measured by Femtosecond Time-Resolved Resonance CARS
By V.F. Kamalov, R. Inaba, and K. Yoshihara (With 1 Figure) 87

Excited States Dynamics of the Special Pair Dimer
By P.O.J. Scherer and S.F. Fischer (With 4 Figures) 89

Creation of an Anti-Wavepacket in a Rydberg Atom
By L.D. Noordam, H. Stapelfeldt, D.I. Duncan, and T.F. Gallagher (With 3 Figures) 92

Squeezing of the Molecular Vibrations by Femtosecond Laser Pulses
By A.V. Vinogradov and J. Janszky (With 1 Figure) 95

Part III Spectroscopy and Advances in Measurements

Spectroscopic Applications of Phase-Locked Femtosecond Pulses
By N.F. Scherer, M. Cho, L.D. Ziegler, M. Du, A. Matro, J. Cina, and G.R. Fleming (With 5 Figures) 99

Use of Piecewise Phase-Swept Pulses to Counteract Inhomogeneous Decay in Wave Packet Interferometry
By L.W. Ungar, A. Matro, and J.A. Cina (With 1 Figure) 105

Ultrafast Nonlinear Spectroscopy with Chirped Optical Pulses
By E.T.J. Nibbering, F. de Haan, D.A. Wiersma, and K. Duppen (With 2 Figures) 107

Multiple Excitation Pulse, Multiple Probe Pulse Femtosecond Spectroscopy
By G.P. Wiederrecht, W. Wang, K.A. Nelson, A.M. Weiner, and D.E. Leaird (With 2 Figures) 110

Stimulated Emission Pumping and Selective Excitation by Adiabatic Passage with Frequency-Modulated Picosecond Laser Pulses
By J.S. Melinger, A. Hariharan, S.R. Gandhi, and W.S. Warren (With 2 Figures) 113

A Subpicosecond Optical Sampling System
By J.D. Kafka, J.W. Pieterse, and M.L. Watts (With 2 Figures) 116

Femtosecond Sagnac Interferometry
By J.-C. Diels, P. Dorn, M. Lai, W. Rudolph, and X.M. Zhao (With 3 Figures) 120

Femtosecond Time-Gated Imaging of Translucent Objects Hidden in Highly Scattering Media
By K.M. Yoo, B.B. Das, F. Liu, Q. Xing, and R.R. Alfano (With 2 Figures) 124

Femtosecond Waveform Processing via Spectral Holography
By A.M. Weiner, D.E. Leaird, D.H. Reitze, and E.G. Paek (With 4 Figures) 128

The Chronocyclic Representation of Ultrashort Light Pulses
By J. Paye (With 4 Figures) 133

Femtosecond Pulse Phase Measurement by Spectrally Resolved Up-Conversion
By J.-P. Foing, J.-P. Likforman, and M. Joffre (With 3 Figures) 136

Single-Shot Measurement
of the Intensity and Phase of a Femtosecond Pulse
By D.J. Kane and R. Trebino (With 4 Figures) 138

Two-Photon Interference Measurement of Ultrafast Laser Pulses
By M. Matsuoka, Y. Miyamoto, T. Kuga, M. Baba, and Y. Li
(With 2 Figures) 140

Picosecond Single-Shot Pulse-Shape Measurement
by Stochastic Sampling of Detected Photon Times
By N. Adams, C. Bovet, E. Rossa, and A. Simonin (With 1 Figure) 142

Integrated Devices for Single Picosecond Pulse Measurements
By V. Gerbe, M. Cuzin, M.C. Gentet, and J. Lajzerowicz
(With 3 Figures) 145

The C850X Ultrafast Streak Camera: An Instrument to Study Spatially
and Temporally Subpicosecond Laser–Matter Interaction
By A. Mens, R. Sauneuf, D. Schirmann, R. Verrecchia, P. Audebert,
J.C. Gauthier, J.P. Geindre, A. Antonetti, J.P. Chambaret, G. Hamoniaux,
and A. Mysyrowicz (With 2 Figures) 147

Distortion of a 6 fs Pulse in the Focus of a BK7 Lens
By Zs. Bor and Z.L. Horváth (With 1 Figure) 150

Part IV **Tools: Sources and Amplifiers**

Modelocking, Stabilizing, and Starting Ultrashort Pulse Lasers
By E.P. Ippen (With 4 Figures) 155

17 fs Pulses from a Mode-Locked Ti:Sapphire Laser
By C.P. Huang, M.T. Asaki, S. Backus, H. Nathel, H.C. Kapteyn,
and M.M. Murnane (With 2 Figures) 160

Design Considerations for Femtosecond Ti:Sapphire Oscillators
By Ch. Spielmann, P.F. Curley, T. Brabec, E. Wintner, A.J. Schmidt,
and F. Krausz (With 3 Figures) 163

Self-Mode-Locked Cr^{3+}:$LiCaAlF_6$ and Cr^{3+}:$LiSrAlF_6$ Lasers
By A. Miller, P. Li Kam Wa, B.H.T. Chai, J.M. Evans, and W. Sibbett
(With 2 Figures) 166

Sub-50 fs Pulse Generation
from a Self-Starting CW Passively Mode-Locked Cr:$LiSrAlF_6$ Laser
By N.H. Rizvi, P.M.W. French, and J.R. Taylor (With 2 Figures) 169

CW Krypton-Laser Pumped Cr^{3+}:$LiSrAlF_6$ and Cr^{3+}:$LiSr_{0.8}Ca_{0.2}AlF_6$
Crystals Produce 150 fs Mode-Locked Pulses
By A. Miller, P. Li Kam Wa, H.S. Wang, S.L. Ayres, E.W. Van Stryland,
and B.H.T. Chai (With 3 Figures) 172

60-fs Chromium-Doped Forsterite (Cr^{4+}:Mg_2SiO_4) Laser
By A. Seas, V. Petričević, and R.R. Alfano (With 3 Figures) 174

Femtosecond Pulses from Nd:Glass Lasers
By A.J. Schmidt, M.H. Ober, M. Hofer, M.E. Fermann, F. Krausz, T. Brabec, Ch. Spielmann, and E. Wintner (With 3 Figures) 177

A Diode-Pumped Picosecond Oscillator at 1053 nm
By I.P. Mercer, Z. Chang, M.R.G. Miller, C.N. Danson, C.B. Edwards, and M.H.R. Hutchinson (With 3 Figures) 182

A New Intracavity Antiresonant Semiconductor Fabry-Perot Passively Mode-Locks Nd:YLF and Nd:YAG Lasers
By U. Keller, D.A.B. Miller, G.D. Boyd, T.H. Chiu, J.F. Ferguson, and M.T. Asom (With 3 Figures) 184

CW Mode-Locked Singly-Resonant Optical Parametric Oscillator Pumped by a Ti:Sapphire Laser
By A. Nebel, U. Socha, and R. Beigang (With 1 Figure) 187

70 fs, High-Average Power, CW Infrared Optical Parametric Oscillator
By G. Mak, Q. Fu, and H.M. van Driel (With 2 Figures) 190

Femtosecond Intracavity Dispersion Measurements
By W.H. Knox (With 2 Figures) 192

Time Synchronization Measurements Between Two Self-Modelocked Ti:Sapphire Lasers
By D.E. Spence, W.E. Sleat, J.M. Evans, W. Sibbett, and J.D. Kafka (With 2 Figures) 194

Femtosecond Synchronous Pumping of Dye Lasers with <100 fs Jitter
By W.H. Knox and F.A. Beisser (With 2 Figures) 196

Development of High Average Power Femtosecond Amplifiers Based on Ti:, Cr: and Nd:Doped Materials
By J. Squier, S. Coe, G. Mourou, D. Harter, and F. Salin 198

Femtosecond Pulse Amplification and Continuum Generation at >250 kHz with a Ti:Sapphire Regenerative Amplifier
By T.B. Norris (With 4 Figures) 200

Millijoule Femtosecond Pulse Amplification in Ti:Al_2O_3 at Multi-kHz Repetition Rates
By F. Salin, J. Squier, G. Mourou, and G. Vaillancourt (With 4 Figures) 203

High Repetition Rate CW Pumped Cr:LiSAF Regenerative Amplifier
By F. Balembois, P. Georges, F. Salin, G. Roger, and A. Brun (With 4 Figures) 206

18 fs Pulse Generation
by a Single Excimer-Laser-Pumped Pulsed Dye Laser
By P. Simon, C. Jordan, and S. Szatmari (With 2 Figures) 209

Monolithic CPM Diode Lasers
By M.C. Wu, Y.K. Chen, T. Tanbun-Ek, and R.A. Logan
(With 5 Figures) 211

Ultrashort Pulse Generation from High-Power Arrays
Using Intracavity Nonlinearities
By L.Y. Pang, J.G. Fujimoto, and E.S. Kintzer (With 3 Figures) 217

100-Gbps Response of Microcavity Lasers
By H. Yokoyama, Y. Nambu, and T. Shimizu (With 2 Figures) 220

Sequential Laser Emission
in Multiple Quantum Well Vertical-Cavity Structures
By C. Tanguy, J.-L. Oudar, B. Sermage, and R. Azoulay
(With 2 Figures) 222

Experimental Analysis of Gain Modulation
in Sub-Picosecond (~0.45 ps) Mode-Locked Laser Diodes
By N. Stelmakh, J.-M. Lourtioz, and D. Pascal (With 3 Figures) 224

Generation of Stable Pulse Trains
with a Passively Modelocked Er-Fiber Laser
By M.E. Fermann, M.J. Andrejco, Y. Silberberg, and A.M. Weiner
(With 4 Figures) 227

Generation of Pairs of Solitons
in an All-Fibre, Femtosecond Soliton Source
By D.J. Richardson, V.V. Afanasjev, A.B. Grudinin, and D.N. Payne
(With 5 Figures) 229

Nonlinear Loop Mirrors in Fiber Lasers
By I.N. Duling III, C.J. Chen, P.K. Wai, and C.R. Menyuk
(With 4 Figures) 232

Temporal Characteristics of the Ytterbium–Erbium Figure-8 Laser
By I.Yu. Khrushchev, A.B. Grudinin, and E.M. Dianov
(With 3 Figures) 235

Generation of 1.7 ps Solitons by Amplification of Pulses from a Laser
Diode with Saturable Absorber in an Erbium-Doped Fibre
By I.Yu. Khrushchev, A.B. Grudinin, E.M. Dianov, D.V. Kuksenkov,
and E.L. Portnoy (With 3 Figures) 237

Part V **High Intensity and Nonlinear Effects**

Generation of Ultra-Intense Pulses and Applications
By G. Mourou (With 1 Figure) 241

Generation of 50 TW Femtosecond Pulses in a Nd-Glass Chain
By C. Rouyer, E. Mazataud, I. Allais, A. Pierre, and S. Seznec
(With 2 Figures) 248

All-Solid Femtosecond Oscillator–Amplifier Laser Chain
with 100 mJ per Pulse
By C. Le Blanc, G. Grillon, J.P. Chambaret, G. Boyer, M. Franco,
A. Mysyrowicz, and A. Antonetti (With 1 Figure) 251

Development of a High Intensity Femtosecond LiSAF Laser
By M.C. Richardson, P. Beaud, B.H.T. Chai, E. Miesak, Y.-F. Chen,
and V. Yanovsky (With 2 Figures) 253

Contrasted Behaviors of Stark-Induced Resonances
in Multiphoton Ionization of Krypton
By E. Mevel, R. Trainham, J. Breger, G. Petite, P. Agostini,
J.P. Chambaret, A. Migus, and A. Antonetti (With 1 Figure) 255

Phase-Dependent Ionization Using an Intense Two-Color Light Field
By D. Schumacher, M.P. de Boer, H.G. Muller, R.R. Jones,
and P.H. Bucksbaum (With 2 Figures) 257

Stabilization of Atoms in Ultra-Intense Laser Pulses: A Classical Model
By A. Maquet, T. Ménis, R. Taïeb, and V. Véniard (With 1 Figure) 259

Inertially Confined Molecular Ions
By M. Laberge, P. Dietrich, and P.B. Corkum (With 2 Figures) 261

A Femtosecond Lightning Rod
By X.M. Zhao, C.Y. Yeh, J.-C. Diels, and C.Y. Wang
(With 2 Figures) 264

Plasma Physics with Ultra-Short and Ultra-Intense Laser Pulses
By T.W. Johnston, Y. Beaudoin, M. Chaker, C.Y. Côté, J.C. Kieffer,
J.P. Matte, H. Pépin, C.Y. Chien, S. Coe, G. Mourou, and D. Umstadter
(With 1 Figure) 267

X-Rays Generated by Femtosecond Laser-Produced Plasmas
By J.P. Geindre, P. P. Audebert, A. Rousse, F. Falliès, J.C. Gauthier,
A. Mysyrowicz, G. Grillon, J.P. Chambaret, A. Antonetti, A. Mens,
R. Verrecchia, R. Sauneuf, and P. Schirman (With 2 Figures) 272

K-Shell Emission from 100 fs Laser-Produced Plasmas
Created from Porous Aluminum Targets
By R. Shepherd, D. Price, B. White, S. Gordan, A. Osterheld, R. Walling,
D. Slaughter, and R. Stewart (With 2 Figures) 275

Kilovolt X-Ray Emission from Femtosecond Laser-Produced Plasmas
By G. Jenke, H. Schüler, T. Engers, D. von der Linde, I. Uschmann,
E. Förster, and K. Gäbel (With 1 Figure) 278

Ultrafast Spectroscopy of Plasmas
Generated by Superintense Femtosecond Laser Pulses
By D. von der Linde, H. Schüler, H. Schulz, and T. Engers
(With 3 Figures) 280

Picosecond Soft-X-Ray Pulse Length Measurement
by Pump–Probe Absorption Spectroscopy
By M.H. Sher, U. Mohideen, H.W.K. Tom, O.R. Wood II,
G.D. Aumiller, D.L. Windt, W.K. Waskiewicz, J. Sugar, T.J. McIlrath,
and R.R. Freeman (With 4 Figures) 283

Photon Acceleration via Laser-Produced Ionization Fronts
By R.L. Savage Jr., R.P. Brogle, W.B. Mori, and C. Joshi
(With 5 Figures) 286

Propagation of Intense Laser Pulses in Plasmas
By E. Esarey, P. Sprangle, J. Krall, and G. Joyce (With 1 Figure) 290

Ponderomotive Steepening in Short-Scale-Length Laser-Plasmas
By D. Umstadter and X. Liu (With 2 Figures) 293

Possibility of Experimental Studies of Nonlinear Quantum
Electrodynamics Effects Using High Power Ultrashort Laser Pulses
By P.G. Kryukov (With 1 Figure) 296

Soliton-Like Self-Trapping of Three-Dimensional Patterns
By A. Barthelemy, C. Froehly, M. Shalaby, P. Donnat, J. Paye,
and A. Migus (With 9 Figures) 299

Physical Origins of the Spectral Continuum:
Self-Focusing, Self-Trapping and Cerenkov Radiation
By F. Salin, J. Watson, J.-F. Cormier, P. Georges, and A. Brun
(With 2 Figures) 306

Diffraction and Focussing of Spectral Energy in a Two-Photon Process
By B. Broers, L.D. Noordam, and H.B. van Linden van den Heuvell
(With 3 Figures) 309

Efficient Raman Conversion of Femtosecond UV Light Pulses
By K.A. Stankov and Y.-W. Lee (With 1 Figure) 311

Organic Crystalline Fiber
for Efficient Compression of Femtosecond Laser Pulses
By M. Yamashita (With 1 Figure) 313

Nonlinear Temporal Diffraction in Optical Fibers
By G.R. Boyer, M.K. Jackson, J. Paye, M.A. Franco, and A. Mysyrowicz
(With 3 Figures) 315

Generation of a Soliton Pulse Train in an Optical Fibre
Using Two CW Single-Frequency Diode Lasers
By S.V. Chernikov, J.R. Taylor, P.V. Mamyshev, and E.M. Dianov
(With 2 Figures) 318

Experimental Investigation of Dark Solitons Interaction
By Ph. Emplit, J.-P. Hamaide, and M. Haelterman (With 3 Figures) 320

Femtosecond Pulse Propagation in Erbium-Doped Single-Mode Fibers
By J.M. Hickmann, A.S.L. Gomes, C.B. de Araújo,
and A.S. Gouveia-Neto (With 3 Figures) 323

Compression of Pulses from Soliton Fibre Lasers
in a Dispersion-Decreasing Fibre
By S.V. Chernikov, D.J. Richardson, E.M. Dianov, and D.N. Payne
(With 4 Figures) 325

Part VI **Metals, Surfaces and Materials**

Observation of the Thermalization of Electrons in a Metal
Excited by Femtosecond Optical Pulses
By W.S. Fann, R. Storz, H.W.K. Tom, and J. Bokor
(With 2 Figures) 331

Femtosecond Thermionic Emission:
Experiment, Analytical Theory, and Particle Simulations
By M.C. Downer, D.M. Riffe, X.Y. Wang, J.L. Erskine, D.L. Fisher,
T. Tajima, and R.M. More (With 2 Figures) 335

Electron–Electron Dynamics Observed in Femtosecond Thermoreflection
Measurements on Noble Metals
By R.H.M. Groeneveld, R. Sprik, and Ad. Lagendijk (With 2 Figures) .. 338

Inversion of Single- and Two-Photon Photoelectric Sensitivities of Metals
in the Femtosecond Range
By J.P. Girardeau-Montaut, C. Girardeau-Montaut, S.D. Moustaïzis,
and C. Fotakis (With 1 Figure) 340

Femtosecond Relaxation of Plasma Excitations in Silver Films
By R.A. Höpfel, D. Steinmüller-Nethl, F.R. Aussenegg, and A. Leitner
(With 3 Figures) 342

Femtosecond Free Induction Decay
of Metal Surface Adsorbate Vibrations
By J.C. Owrutsky, J.P. Culver, M. Li, Y.R. Kim, M.J. Sarisky,
M.S. Yeganeh, R.M. Hochstrasser, and A.G. Yodh (With 1 Figure) 345

Observation of Laser-Induced Desorption of CO from Cu(111)
with 100 fs Time-Resolution
By J.A. Prybyla, H.W.K. Tom, and G.D. Aumiller (With 2 Figures) 347

Femtosecond Desorption of Molecular Oxygen from Pt(111)
By F.-J. Kao, D.G. Busch, D. Gomes da Costa, D. Cohen, and W. Ho
(With 1 Figure) 350

Femtosecond Carrier Dynamics in Solid C_{60} Films
By S.D. Brorson, M.K. Kelly, U. Wenschuh, R. Buhleier, and J. Kuhl
(With 4 Figures) 354

The Role of Covalency in Femtosecond Time-Resolved Reflectivity
of Hydrodynamically Expanding Solid Surfaces
By X.Y. Wang, H.Y. Ahn, and M.C. Downer (With 1 Figure) 357

Ultrafast Formation Processes of Self-Trapped Excitons
in Alkali Iodide Crystals under Band-to-Band Excitation
By T. Tokizaki, S. Iwai, T. Shibata, A. Nakamura, K. Tanimura,
and N. Itoh (With 2 Figures) 360

Femtosecond Self-Trapping of Interacting Electron–Hole Pairs in α-SiO_2
By W. Joosen, S. Guizard, P. Martin, G. Petite, P. Agostini,
A. Dos Santos, G. Grillon, J.P. Chambaret, D. Hulin, A. Migus,
and A. Antonetti (With 4 Figures) 362

Ultrafast Soft Mode Dynamics in Ferroelectric Crystals
By G.P. Wiederrecht, T.P. Dougherty, and K.A. Nelson
(With 3 Figures) 365

Temporal Domain Study of the Phase Transition in $PbTiO_3$:
A_1 Symmetry Investigation
By D.P. Kien, J.C. Loulergue, and J. Etchepare (With 2 Figures) 368

Femtosecond Transient Absorption Measurements
on Low Band Gap Thiophene Polymers
By A. Cybo-Ottoné, M. Nisoli, V. Magni, S. De Silvestri, O. Svelto,
G. Zerbi, and R. Tubino (With 2 Figures) 370

Effects of Crosslinking in Host Polymer
on Picosecond Optical Dephasing of Doped Dye Molecules
By S. Nakanishi, S. Fujiwara, M. Kawase, and H. Itoh
(With 3 Figures) 372

Ultrafast Relaxation of Exciton and Soliton–Antisoliton Pair
in One-Dimensional Conjugated Polymers
By T. Kobayashi, M. Yoshizawa, S. Takeuchi, and A. Yasuda
(With 2 Figures) 376

Polarization-Dependent Femtosecond Dynamics
of MBE-Grown Phthalocyanine Organic Thin Films
By Sandalphon, V.S. Williams, K. Meissner, N.R. Armstrong,
and N. Peyghambarian (With 3 Figures) 379

Detection of a New Strongly-Coupled Vibration Mode
During the Exciton Bleaching of Polydiacetylene
By J.M. Nunzi, C. Hirlimann, and J.F. Morhange (With 1 Figure) 381

Pressure-Induced Vibrational Relaxation and Electronic Dephasing in Molecular Crystals
By E.L. Chronister and R.A. Crowell (With 3 Figures) 384

Ultrafast Reversible Phase Changes for Optical Recording
By J. Solís, C.N. Afonso, F. Catalina, and C. Kalpouzos
(With 1 Figure) 387

Picosecond Transient Absorption and Fluorescence Emission Studies of C_{60} and C_{70} in Solution
By D. Kim, Y.D. Suh, S.K. Kim, and M. Lee (With 2 Figures) 389

Part VII **Semiconductors, Confinement and Opto-Electronics**

Transient Absorption-Edge Singularities in GaAs
By D. Hulin, J.-P. Foing, M. Joffre, M.K. Jackson, J.-L. Oudar, C. Tanguy, and M. Combescot (With 3 Figures) 395

Nonthermal Distribution of Electrons in GaAs
By D. Snoke and W.W. Rühle (With 1 Figure) 399

Femtosecond Carrier–Carrier Interaction in GaAs
By T. Gong, K.B. Ucer, L.X. Zheng, G.W. Wicks, J.F. Young, P.J. Kelly, and P.M. Fauchet (With 4 Figures) 402

Quantum Beats versus Polarization Interference: An Experimental Distinction
By M. Koch, J. Feldmann, G. von Plessen, E.O. Göbel, P. Thomas, and K. Köhler (With 1 Figure) 405

Plasmon–Phonon Coupling and Hot Carrier Relaxation in GaAs and Low-Temperature-Grown GaAs
By R.I. Devlen, J. Kuhl, and K. Ploog (With 2 Figures) 408

Femtosecond Carrier–Carrier Interaction Dynamics in Doped GaAs
By T. Furuta and A. Yoshii (With 1 Figure) 410

Femtosecond Carrier Kinetics in Low-Temperature-Grown GaAs
By X.Q. Zhou, H.M. van Driel, A.P. Heberle, W.W. Rühle, and K. Ploog (With 2 Figures) 412

Transient Anisotropic Luminescence and Long-Living Polarization of an Optically Excited Dense Electron–Hole Plasma
By A.L. Ivanov and H. Haug (With 2 Figures) 414

Hot Hole Capture by Shallow Acceptors in p-Type GaAs Studied by Picosecond Infrared Spectroscopy
By A. Lohner, M. Woerner, T. Elsaesser, and W. Kaiser
(With 2 Figures) 416

Ultrafast Dephasing and Interference of Coherent Phonons in GaAs
By W. Kütt, T. Pfeifer, T. Dekorsy, and H. Kurz (With 2 Figures) 418

Femtosecond, Electronically-Induced Disordering of GaAs
By J.-K. Wang, Y. Siegal, P.N. Saeta, N. Bloembergen, and E. Mazur
(With 2 Figures) 420

Laser-Induced Ultrafast Order–Disorder Transitions in Semiconductors
By K. Sokolowski-Tinten, J. Bialkowski, and D. von der Linde
(With 1 Figure) 422

Femtosecond Carrier Dynamics in InGaAsP Optical Amplifiers
By J. Mark and J. Mørk (With 1 Figure) 424

Ultrafast Nonlinear Refraction in Semiconductor Laser Amplifiers
By M. Sheik-Bahae and E.W. Van Stryland (With 3 Figures) 426

Femtosecond Luminescence Spectroscopy of Indium Phosphide
By E. Fazio and G.M. Gale (With 2 Figures) 429

Dynamics of Excitons Probed by Accumulated Photon Echo
By T. Bouma, P. Vledder, and J.I. Dijkhuis (With 1 Figure) 431

Time-Resolved Measurement of Hot Carrier Cooling Rates
in a-Si:H and a-Ge:H
By M. Wraback and J. Tauc (With 2 Figures) 433

Dephasing of the Short Exciton–Polariton Pulses
in Polar Semiconductors: The Cuprous Chloride Case
By F. Vallée, F. Bogani, and C. Flytzanis (With 3 Figures) 435

Femtosecond Electronic Dynamics of CdSe Nanocrystals
By C.V. Shank, R.W. Schoenlein, D.M. Mittleman, J.J. Shiang,
and A.P. Alivisatos (With 4 Figures) 438

Quantum Beats Spectroscopy of Exciton Spin Dynamics
in GaAs Heterostructures
By S. Bar-Ad and I. Bar-Joseph (With 3 Figures) 443

Evidence of Slow Hole Spin Relaxation
in n-Modulation Doped GaAs/AlGaAs Quantum Well Structures
By Ph. Roussignol, P. Rolland, R. Ferreira, C. Delalande, G. Bastard,
A. Vinattieri, J. Martinez-Pastor, L. Carraresi, M. Colocci, J.F. Palmier,
and B. Etienne (With 1 Figure) 446

Femtosecond Time-Resolved Four-Wave Mixing in GaAs Quantum Wells
By D.S. Kim, J. Shah, T.C. Damen, J.E. Cunningham, W. Schäfer,
and S. Schmitt-Rink (With 4 Figures) 448

Exciton Radiative Lifetimes in GaAs Quantum Wells
By R. Eccleston, J. Kuhl, W.W. Rühle, and K. Ploog
(With 2 Figures) 451

Optical Investigation of Bloch Oscillations
in a Semiconductor Superlattice
By J. Feldmann, K. Leo, J. Shah, D.A.B. Miller, J.E. Cunningham,
T. Meier, G. von Plessen, P. Thomas, and S. Schmitt-Rink
(With 5 Figures) 454

Coherent Pulse Breakup
in Femtosecond Pulse Propagation in Semiconductors
By P.A. Harten, A. Knorr, S.G. Lee, R. Jin, F. Brown de Colstoun,
E.M. Wright, G. Khitrova, H.M. Gibbs, S.W. Koch,
and N. Peyghambarian (With 1 Figure) 458

Absorption Saturation of the Urbach's Tail in Multiple Quantum Wells
By R. Raj, B.G. Sfez, D. Pellat, and J.L. Oudar (With 2 Figures) 460

Photon Echo Polarisation Rules in GaAs Quantum Wells
By R. Eccleston, D. Bennhardt, J. Kuhl, P. Thomas, and K. Ploog
(With 3 Figures) 463

Observation of Many-Body Effects in the Femtosecond Temporal Profile
of Quasi-2D Exciton Free-Induction Decay
By S. Weiss, M.-A. Mycek, J.-Y. Bigot, S. Schmitt-Rink,
and D.S. Chemla (With 3 Figures) 466

Radiative Recombination of Free Excitons in GaAs Quantum Wells
By B. Sermage, K. Satzke, C. Dumas, N. Roy, B. Deveaud, F. Clerot,
and D.S. Katzer (With 4 Figures) 472

Field-Enhanced GaAs/AlGaAs Waveguide Saturable Absorbers
By J.R. Karin, D.J. Derickson, R.J. Helkey, J.E. Bowers,
and R.L. Thornton (With 2 Figures) 475

Picosecond Excitonic Nonlinearities in the Presence of Disorder
By S.T. Cundiff and D.G. Steel (With 3 Figures) 478

Fast Optical Nonlinearities in Semiconductor Quantum Dots
By G. Tamulaitis, R. Baltramiejūnas, S. Pakalnis, and A.I. Ekimov
(With 2 Figures) 482

Terahertz Radiation from Coherent Electron Oscillations
in a Double-Quantum-Well Structure
By H.G. Roskos, M.C. Nuss, J. Shah, K. Leo, D.A.B. Miller,
S. Schmitt-Rink, and K. Köhler (With 3 Figures) 484

Optical Generation of Terahertz Pulses from Polarized Excitons
in Quantum Wells
By P.C.M. Planken and M.C. Nuss (With 3 Figures) 487

Generation of High-Power Single-Cycle Picosecond Radiation
By D.R. Dykaar, R.R. Jones, D. You, D. Schumacher,
and P.H. Bucksbaum (With 3 Figures) 490

Transient Electron Transport in GaAs Quantum Wells:
From the Ballistic to the Quasi-Equilibrium Regime
By W. Sha, J. Rhee, and T.B. Norris (With 4 Figures) 493

A Novel Free-Standing Absolute-Voltage Probe
with 2.3-Picosecond Resolution and 1-Microvolt Sensitivity
By J. Kim, S. Williamson, J. Nees, and S. Wakana
(With 3 Figures) 496

Picosecond Pseudomorphic AlGaAs/InGaAs MODFET Large-Signal
Switching Measured by Electro-Optic Sampling
By M.K. Jackson, M.Y. Frankel, J.F. Whitaker, G.A. Mourou, D. Hulin,
A. Antonetti, M. Van Hove, W. De Raedt, P. Crozat, and H. Hafdallah
(With 3 Figures) 500

Ultrafast Decay of Photodiffractive Gratings in Hetero n-i-p-i's
by Enhanced In-Plane Transport
By A.L. Smirl, D.S. McCallum, A.N. Cartwright, X.R. Huang,
T.F. Boggess, and T.C. Hasenberg (With 2 Figures) 503

Picosecond High-Sensitivity $In_xGa_{1-x}As$ Photodetectors
By S. Gupta, J.F. Whitaker, S.L. Williamson, P. Ho, J.S. Mazurowski,
and J.M. Ballingall (With 2 Figures) 505

An Ultrafast Polarization-Independent All-Optical Demultiplexer
Utilizing Induced-Frequency Shift
By T. Morioka, K. Mori, and M. Saruwatari (With 2 Figures) 508

Electrical Soliton Devices as >100 GHz Signal Sources
By E. Carman, M. Case, M. Kamegawa, R. Yu, K. Giboney,
and M. Rodwell (With 2 Figures) 511

Determination of Photonic Band Gaps and Dispersion
in Two-Dimensional Dielectric Arrays
with Ultrafast Electromagnetic Transients
By W.M. Robertson, G. Arjavalingam, R.D. Meade, K.D. Brommer,
A.M. Rappe, and J.D. Joannopoulos (With 2 Figures) 513

Part VIII **Biology: Primary Dynamics, Electron and Energy Transfer**

Ultrafast Infrared Spectroscopy of Protein Dynamics
By R.M. Hochstrasser, R. Diller, S. Maiti, T. Lian, B. Locke, C. Moser,
P.L. Dutton, B.R. Cowen, and G.C. Walker (With 5 Figures) 517

Ultrafast Near-IR Spectroscopy of Carbonmonoxymyoglobin:
The Dynamics of Protein Relaxation
By M. Lim, T.A. Jackson, and P.A. Anfinrud (With 4 Figures) 522

Energetics and Dynamics of Global Protein Motion
By R.J.D. Miller, J. Deak, S. Palese, M. Pereira, L. Richard, and L. Schilling (With 2 Figures) 525

Investigation of the Reaction Coordinate for Ligand Rebinding in Photoexcited Hemeproteins Using Transient Raman Spectroscopy
By H. Zhu, R. Lingle, Jr., X. Xu, and J.B. Hopkins (With 2 Figures) 528

Resonance Raman Studies of Electronic and Vibrational Relaxation Dynamics in Heme Proteins
By P.M. Champion, J.T. Sage, and P. Li 533

Molecular Processes in the Primary Reaction of Photosynthetic Reaction Centers
By W. Zinth, C. Lauterwasser, U. Finkele, P. Hamm, S. Schmidt, and W. Kaiser (With 3 Figures) 535

Femtosecond Spontaneous Emission Studies of Photosynthetic Bacterial Reaction Centers
By S.J. Rosenthal, M. Du, X. Xie, T.J. DiMagno, M.E. Schmidt, J.R. Norris, and G.R. Fleming (With 1 Figure) 539

Subpicosecond Emission Studies of Bacterial Reaction Centers
By P. Hamm and W. Zinth (With 1 Figure) 541

Picosecond Fluorescence Kinetics of Purple Bacterial Reaction Centers
By M.G. Müller, K. Griebenow, and A.R. Holzwarth (With 2 Figures) .. 543

Primary Radical Pair Formation in Photosystem-Two Reaction Centres
By D.R. Klug, J.R. Durrant, G. Hastings, Q. Hong, D.M. Joseph, J. Barber, and G. Porter (With 3 Figures) 546

Energy Transfer and Primary Charge Separation in Heliobacteria by Picosecond Transient Absorption Spectroscopy
By P.I. van Noort, T.J. Aartsma, and J. Amesz (With 3 Figures) 549

Excitation Energy Transfer in Mutants of *Rb. sphaeroides*: The Effects of Changes in the Core Antenna Size
By L.M.P. Beekman, R.W. Visschers, K.J. Visscher, B. Althuis, W. Barz, D. Oesterhelt, V. Sundström, and R. van Grondelle (With 3 Figures) 552

Femtosecond Excitation Transfer in Allophycocyanin
By A.V. Sharkov, E.V. Khoroshilov, I.V. Kryukov, P.G. Kryukov, T. Gillbro, R. Fischer, and H. Scheer (With 1 Figure) 555

Femtosecond Förster Energy Transfer over 20 Å in Phycoerythrocyanin (PEC) Trimers
By L.O. Palsson, T. Gillbro, A. Sharkov, R. Fischer, and H. Scheer (With 1 Figure) 557

Ultrafast Energy Transfer Within the Light-Harvesting Antenna
of Photosynthetic Purple Bacteria
By K.J. Visscher, V. Gulbinas, R.J. Cogdell, R. van Grondelle, and
V. Sundström (With 2 Figures) 559

Femtosecond Dynamics in Rhodopsin
By T. Kobayashi, M. Taiji, K. Bryl, M. Nakagawa, and M. Tsuda
(With 2 Figures) 562

Subpicosecond Time-Resolved Spectroscopy of Halorhodopsin
and Comparison with Bacteriorhodopsin
By H. Kandori, K. Yoshihara, H. Tomioka, H. Sasabe, and Y. Shichida
(With 3 Figures) 566

Part IX **Chemistry: Electron and Energy Transfer, and Solvation Dynamics**

Femtosecond Intermolecular Electron Transfer:
Dye in Weakly Polar Electron-Donating Solvent
By K. Yoshihara, A. Yartsev, Y. Nagasawa, H. Kandori, A. Douhal,
and K. Kemnitz (With 3 Figures) 571

Ultrafast Studies and Simulations
on Direct Photoinduced Electron Transfer in the Betaines
By A.E. Johnson, N.E. Levinger, G.C. Walker, and P.F. Barbara
(With 3 Figures) 576

Picosecond Infrared Study of Ultrafast Electron Transfer
and Vibrational Energy Relaxation in $[(NC)_5RU^{II}CNRu^{III}(NH_3)_5]^{1-}$
By P.O. Stoutland, S.K. Doorn, R.B. Dyer, and W.H. Woodruff
(With 1 Figure) 579

Ultrafast Studies on Intervalence Charge Transfer
By K. Tominaga, D.A.V. Kliner, J.T. Hupp, and P.F. Barbara
(With 1 Figure) 582

Picosecond Infrared Study of Intramolecular Energy Transfer
in $[(phen)(CO)_3Re^{I}(NC)Ru^{II}(CN)(bpy)_2]^{+}$
By R.B. Dyer, K.A. Peterson, K.C. Gordon, W.H. Woodruff,
J.R. Schoonover, T.J. Meyer, and C.A. Bignozzi (With 1 Figure) 585

Noise-Induced Intramolecular Electron Transfer Processes in Polar Media
By P.O.J. Scherer 587

Femtosecond Proton Transfer
in the Electronic Ground State of Vibrationally Hot Molecules
By T. Elsaesser, W. Frey, and M.T. Portella (With 2 Figures) 589

Solvent Effects on the Fast Proton Transfer of 3-Hydroxyflavone
By B.J. Schwarz, L.A. Peteanu, and C.B. Harris (With 3 Figures) 592

Time-Resolved Charge Separation
in Acceptor-Substituted Anthrylpolyenes
By H. Port, G. Quapil, H.C. Wolf, F. Effenberger, C.-P. Niesert,
R. Buhleier, Z. Gogolak, and J. Kuhl (With 2 Figures) 596

Vibrationally Unrelaxed cis-Stilbene Photoproducts Examined Through
Two-Color UV Pump-Probe Anti-Stokes Raman Spectroscopy
By D.L. Phillips, J.-M. Rodier, and A.B. Myers (With 4 Figures) 598

Vibrational Energy Redistribution and Relaxation
in the Photoisomerization of cis-Stilbene
By R.J. Sension, S.T. Repinec, A.Z. Szarka, and R.M. Hochstrasser
(With 2 Figures) 601

Photoisomerization of cis-Stilbene in Compressed Solvents
By L. Nikowa, D. Schwarzer, J. Troe, and J. Schroeder
(With 2 Figures) 603

Ultrafast Torsional Dynamics in Adsorbates: An SSHG Study
By M.J.E. Morgenthaler and S.R. Meech (With 1 Figure) 606

Barrierless Photochemical Isomerization
By U. Åberg, E. Åkesson, I. Fedchenia, and V. Sundström
(With 2 Figures) 608

Femtosecond Molecular Dynamics in Liquids
By D.A. Wiersma, E.T.J. Nibbering, and K. Duppen
(With 4 Figures) 611

Femtosecond Solvent Dynamics
Studied by Time-Resolved Fluorescence and Transient Birefringence
By S.J. Rosenthal, N.F. Scherer, M. Cho, X. Xie, M.E. Schmidt,
and G.R. Fleming (With 2 Figures) 616

Adiabatic and Nonadiabatic Effects in Solvation Dynamics
By E. Neria and A. Nitzan (With 1 Figure) 618

Excited-State Processes of 7-Azaindole
By M. Négrerie, F. Gai, J.-C. Lambry, J.-L. Martin, and J.W. Petrich
(With 1 Figure) 621

Excited-State Proton Transfer and Hydrogen-Bonding Dynamics in
7-Azaindole: Time-Resolved Fluorescence and Computer Simulation
By C.F. Chapman, T.J. Marrone, R.S. Moog, and M. Maroncelli 624

Transient Hole Burning Studies of Electronic State Solvation:
Phonon and Structural Contributions
By J. Yu, J.T. Fourkas, and M. Berg (With 2 Figures) 626

Subpicosecond Study of the Dynamic Processes
in Push-Pull Styrenes and the Role of Solvation
By P. Hébert, G. Baldacchino, T. Gustavsson, V. Kabelka, P. Baldeck,
and J.-C. Mialocq (With 3 Figures) 628

Picosecond Studies of Charge Transfer States in "Push-Pull" Linear
Diphenyl Polyenes: Experimental Evidence for TICT and Bicimer States
By J.M. Viallet, F. Dupuy, R. Lapouyade, W.Q. Zheng, and C. Rullière
(With 2 Figures) 631

Features of the Dual Fluorescence of 4-N,N-dialkylaminoalkylbenzoates
in Alkanes
By M.C.C. de Lange, D.T. Leeson, A.H. Huizer, and C.A.G.O. Varma
(With 1 Figure) 634

Investigation of Fast Relaxation Processes
in Non-Fluorescent Rhodamine Dyes
By P. Plaza, N.D. Hung, M.M. Martin, Y.H. Meyer, and W. Rettig
(With 1 Figure) 636

Femtosecond Photodissociation of Aromatic Disulfides
Followed by Solvent Relaxation
By N.P. Ernsting (With 4 Figures) 638

Femtosecond Dynamics of C–O Bond Cleavage
of a Spirooxazine Photochromic Reaction
By N. Tamai and H. Masuhara (With 2 Figures) 641

Dynamics of Molecular Rotation at the Air/Water Interface by Time-
Resolved Second-Harmonic Generation
By A. Castro, D. Zhang, and K.B. Eisenthal (With 5 Figures) 644

Energy Relaxation and Redistribution in Large Molecules in Solution on
Ultrafast Time Scales
By C.B. Harris, J.C. King, K.E. Schultz, B.J. Schwartz, and J.Z. Zhang
(With 2 Figures) 650

Photodissociation and Recombination Dynamics of I_2^- in Solution
By J.C. Alfano, D.A.V. Kliner, A.E. Johnson, N.E. Levinger, and
P.F. Barbara (With 3 Figures) 653

Probing the Microscopic Molecular Environment in Liquids
with Femtosecond Fourier-Transform Raman Spectroscopy
By D. McMorrow, S.K. Kim, J.S. Melinger, and W.T. Lotshaw
(With 3 Figures) 656

The Homogeneity of Liquid Phase Vibrational Line Broadening
from Raman Echo Experiments
By L.J. Muller, D. Vanden Bout, and M. Berg (With 2 Figures) 658

Excited State Photoreactions of Chlorine Dioxide in Solution
By R.C. Dunn and J.D. Simon (With 2 Figures) 661

Bimolecular Reactions are Power-Full
By A. Masad, S.Y. Goldberg, D. Huppert, and N. Agmon
(With 4 Figures) 664

Dynamics and Mechanism of Cu-Porphyrin Triplet Quenching
Through Liganding by Oxygen-Containing Solvents
By V.S. Chirvony and R. Gadonas 667

Fast Processes in Liquid Alkane Photolysis
Above the Ionization Threshold
By M. Sander, U. Brummund, K. Luther, and J. Troe (With 1 Figure) . . 669

Index of Contributors 671

Subpicosecond Emission Studies of Bacterial Reaction Centers

P. Hamm and W. Zinth

Institut für medizinische Optik der Ludwig-Maximilians-Universität München, Barbarastr. 16, W-8000 München, Fed. Rep. of Germany

The emission of the electronically excited state of the special pair in the reaction centers of the photosynthetic bacterium Rhodobacter (Rb.) sphaeroides R26.1 and several mutants was observed by upconversion. In all samples, a biexponential decay of the fluorescence emission was observed.

In the primary photosynthetic reaction energy is stored by a charge transfer across a membrane bound pigment protein complex called reaction center (RC). The x-ray structure analysis of RC's from Rb. sphaeroides has shown that the electron carrying pigments are arranged in two branches (A and B) related by an approximate C2-symmetry. It is known that the electron uses predominantly the A branch. By transient absorbance measurements 3 kinetic components were found which could be associated with a sequential reaction model. After electronical excitation of the special pair (P) by a photon the electron is transfered via a bacteriochlorophyll monomer (B_A) in 3.5 ps to a bacteriopheophytin (H_A) in 0.9 ps, and finally to a quinone (Q_A) in 200 ps.

In order to get new and independent information on the first reaction step we investigated fluorescence emission of the electronically excited state P^*. We present data on native RC's from Rb. sphaeroides and from mutants where the tyrosine at position M210 and the phenylalanine L181 were exchanged. In detail, we have investigated (YM210→F), (FL181→Y), and (YM210→F,FL181→Y). The mutations were at symmetry related positions between the special pair and chlorophyll monomer on each branch.

The experiments were based on a femtosecond near infrared laser-amplifier system operating at a repetition rate of 10 Hz. Exitation was performed at a wavelength of 865nm. The fluorescence light at a wavelength of 920 nm was upconverted in a 1mm thick BBO crystal. Uncritical collinear Type II phasematching was used. The time resolution was approximately 400 fs.

The transient absorbance measurements on native RC's in the spectral region of stimulated emission indicated that P^* decays monoexponentially with a time constant of 3.5ps. The results of the emission experiments are plotted in Fig. 1. No data trace follows a monoexponential decay. However, the measurements can be explained well by a biexponential model function with time constants of 2ps-6ps for a faster component and 7ps-26ps for the slower component. The values of the time constants ($\tau 1$, $\tau 2$) and the amplitude ratios (A_2/A_1) are summarized in Table 1.

No other fast time constant is required to explain the experimental data; e.g. the 0.9 ps kinetic component which was observed by transient absorbance measurements in the spectral region of the absorption bands of B_A is not observed in the emission experiment. On the other hand one would expect the 0.9 ps kinetic if it reflects an energy relaxation process within P^*. Therefore our finding supports the stepwise electron transfer model where the 0.9 ps kinetic is related to the transfer step from B_A to H_A.

Within the scope of nonadiabatic electron transfer theory the observation of an additional time constant (the 3.5ps kinetic splits into two kinetics) indicates that a new intermediate state has to be considered. Although we can not finally rule out other

Springer Series in Chemical Physics, Vol. 55 **Ultrafast Phenomena VIII**
Editors: J.-L. Martin · A. Migus · G.A. Mourou · A.H. Zewail

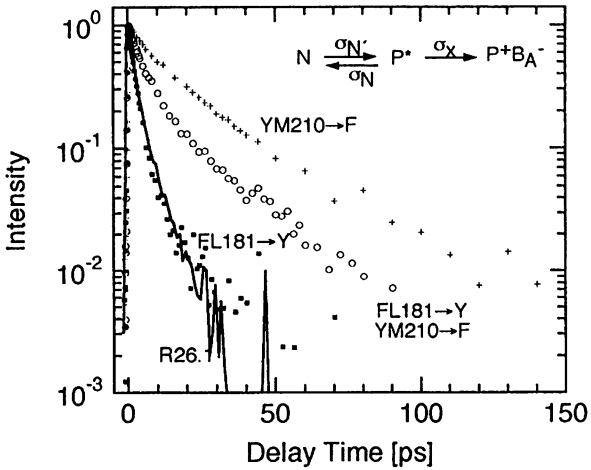

Fig.1: The emission experiments on RC's of R26.1 and of the mutants (YM210→F), (FL181→Y), and (YM210→F,FL181→Y).

Table 1:

	τ_1 [ps]	τ_2 [ps]	A_2/A_1	$1/\sigma_x$ [ps]	$1/\sigma_N$ [ps]	$1/\sigma_N'$ [ps]
R26.1	2.3	7	0.25	3.2	13	4.8
YM210→F	6.1	26	1.37	18	29	9.0
FL181→Y	2.1	15	0.06	2.8	10	11
YM210→F,FL181→Y	3.5	18	0.59	8.8	11	7.1

reaction models we want to focus on the model which is shown as an insert in Fig 1. The model contains a "parking state" N coupled to P^*. The reaction rates σ_x, σ_N, and σ_N' can be evaluated directly from the measured time constants and amplitude ratios and are summarized in Table 1. It can be seen, that a replacement of a phenylalanine by a tyrosine tends to speed up the reaction into the direction of the branch where the tyrosine is introduced.

A reevaluation of our former absorbance measurements taking into account the time constants given above allows us to compute the spectral properties of state N to be similar to those expected for a P^+B^- state. This leads to the conclusion, that the "parking state" N may be $P^+B_B^-$ were the electron is transiently brought on the inactive, the B branch.

Acknowledgement: The experiments were performed in collaboration with W.Kaiser, H.Scheer, D.Oesterhelt and K.Gray